



# A novel method for synthesis of phosphomolybdic acid-modified Pd/C catalysts for oxygen reduction reaction

Mingyuan Zhu<sup>a,b</sup>, Xiaoling Gao<sup>a</sup>, Guangqin Luo<sup>a</sup>, Bin Dai<sup>a,b,\*</sup>

<sup>a</sup>School of Chemistry and Chemical Engineering of Shihezi University, Shihezi Xinjiang 832003, China

<sup>b</sup>Key Laboratory for Green Processing of Chemical Engineering of Xinjiang Bingtuan, Shihezi Xinjiang 832003, China

## H I G H L I G H T S

- ▶ A novel method is proposed to synthesizing Pd/HPMo–PAN–C catalyst.
- ▶ Pd/HPMo–PAN–C catalyst exhibited high catalytic activity for oxygen reduction reaction.
- ▶ HPMo species increase the ORR electron transfer number of Pd nano-particles.
- ▶ Pd/HPMo–PAN–C catalyst is very stable in acidic medium even though HPMo is soluble.

## A R T I C L E I N F O

### Article history:

Received 6 October 2012

Accepted 8 October 2012

Available online 17 October 2012

### Keywords:

Oxygen reduction reaction

Methanol tolerance

Heteropolyacids

Palladium catalyst

Stability

Activity

## A B S T R A C T

This manuscript reports a convenient method for immobilizing phosphomolybdic acid (HPMo) on polyaniline (PAN-) functionalized carbon supports. The obtained HPMo–PAN–C sample is used as the support to prepare a Pd/HPMo–PAN–C catalyst. The samples are characterized by Fourier transform infrared spectroscopy, transmission electron microscopy and X-ray diffraction analysis. The results suggest that HPMo retains its Keggin structure and that the presence of HPMo reduces the average particle size of the Pd nano-particles in the obtained Pd/HPMo–PAN–C catalyst. Electro-chemical measurements in 0.5 M HClO<sub>4</sub> solution reveal that the Pd/HPMo–PAN–C catalyst has higher catalytic activity for oxygen reduction reactions than does a Pd/C catalyst prepared using a similar procedure. The stability of the Pd/HPMo–PAN–C catalyst is evaluated by multiple-cycle voltammetry techniques; the mass catalytic activity decreases by only 10% after 100 scanning cycles.

© 2012 Elsevier B.V. All rights reserved.

## 1. Introduction

Direct methanol fuel cells (DMFCs) have attracted much attention in recent years as potential clean and mobile power sources. However, the cathode catalyst currently used in DMFCs suffers from many technical problems. Many non-precious metal combinations, including carbides, chalcogenides, and nitrides, have been applied as a cathode catalyst instead of Pt/C to reduce the cost of the DMFC catalyst. However, these catalysts exhibit low activity and poor stability for oxygen reduction reaction (ORR), which restricts their ultimate applicability for DMFCs.

Pd/C catalysts are considerably less expensive than Pt/C catalysts and exhibit remarkable catalytic activity for ORR with excellent methanol tolerance; thus, carbon-supported Pd and PdM [1,2]

(M = Fe, Co et al.) catalysts have been widely applied as cathode catalysts for DMFCs and proton exchange membrane fuel cells (PEMFCs). In these PdM catalysts, Pd was alloyed with transition metals, which decreased the Pd–Pd bond distance, lowering the energy of the electron in the Pd d-orbitals. The enhanced catalytic activity was attributed to the decrease in the Gibbs free energy in the ORR electron transfer steps as a result of the alloying effect. However, carbon-supported PdM catalysts tend to suffer from stability issues because the non-noble transition metal dissolves in acidic medium, which decreases the ORR stability of these catalysts in H<sub>2</sub>SO<sub>4</sub> or HClO<sub>4</sub> solutions.

Heteropolyacids (HPAs) are capable of fast reversible multi-electron transfers and thus have been investigated as catalyst additives for methanol oxidation reaction (MOR) and ORR in DMFCs. Seo et al. [3] deposited phosphomolybdic acid (HPMo) on Pt/CNTs catalysts; the obtained catalysts exhibited catalytic mass activity for the electro-oxidation of methanol that was at least 50% greater than that of Pt/CNTs. The authors of that study proposed that the presence of HPMo in the catalyst facilitated the

\* Corresponding author. School of Chemistry and Chemical Engineering of Shihezi University, Shihezi Xinjiang 832003, China. Tel.: +86 993 2057270; fax: +86 993 2057210.

E-mail address: [db\\_tea@shzu.edu.cn](mailto:db_tea@shzu.edu.cn) (B. Dai).

electro-oxidation of intermediate species, such as the CO species produced in the MOR process. Wang et al. [4] found that the catalytic activity of HPA-assembled Pt/C for ORR was much higher than that of pure Pt/C. HPA-assembled Pt/C catalyst was assumed to exhibit high catalytic activity towards the reduction of  $\text{H}_2\text{O}_2$  produced in ORR via a bifunctional mechanism in which Pt was active and HPA induced the reductive decomposition of the  $\text{H}_2\text{O}_2$  intermediate [5]. Although HPA can enhance catalytic activity, the stability of HPA-assembled catalysts is still poor due to the high solubility of HPA in water. To improve the stability of the catalysts, HPA must be immobilized on the surface of the carbon support. Wang et al. [6] reported that HPA can be effectively immobilized on CNT via the electrostatic force between the negatively charged HPA and positively charged functionalized CNTs. However, this electro-chemical synthesis method is complicated and expensive, limiting its potential application in DMFCs.

This paper reports a convenient method for immobilizing HPMo on XC-72R carbon supports to improve the ORR catalytic activity and stability of the Pd catalyst. Fourier transform infrared spectroscopy (FTIR), transmission electron microscopy (TEM) and X-ray diffraction (XRD) experiments were performed to characterize the physical structure of the obtained catalyst, and the catalytic activity and stability of the catalyst were evaluated by electro-chemical techniques.

## 2. Experimental

### 2.1. Catalyst preparation

Approximately 100 mg of commercial Vulcan XC-72R carbon support (Cabot Corp.,  $S_{\text{BET}} = 250 \text{ m}^2 \text{ g}^{-1}$ ) was suspended in 0.5 M HCl solution by ultrasonication in the presence of 1 ml of aniline, followed by the addition of  $(\text{NH}_4)_2\text{S}_2\text{O}_8$  as an oxidant to form polyaniline (PAN). After stirring for 12 h, the solution was filtered, washed and dried at  $60^\circ\text{C}$ . The obtained powder was impregnated in 1 mM HPMo solution for 5 h, and the solution was then filtered, washed, and dried. The as-synthesized sample was denoted as HPMo–PAN–C. Approximately 33.4 mg of  $\text{PdCl}_2$  was dissolved in 50 ml of ethylene glycol with vigorous stirring, followed by the addition of 80 mg of HPMo–PAN–C. After 30 min of stirring, 5 ml of aqueous NaOH solution (1 M) was added to adjust the pH value to 11. Next, the mixture was slowly heated to  $110^\circ\text{C}$  and maintained at this temperature for 3 h. After cooling to ambient temperature, the mixture was filtrated, washed and dried. The Pd loading of the as-synthesized Pd/HPMo–PAN–C catalyst was 20 wt.%. Using a similar procedure, Pd/C with 20 wt.% Pd loading was also prepared for catalytic activity comparison.

### 2.2. Catalyst characterization

FTIR and TEM measurements were recorded on an Avatar 360 ESP FTIR spectrometer and a Tecnai F30 field emission transmission electron microscope, respectively. The XRD data were obtained using a Bruker Advanced D8 X-ray power diffractometer with a Cu K $\alpha$  radiation source and a Ni filter.

### 2.3. Electro-chemical catalyst measurements

The ORR catalytic activity was evaluated with a CHI760D measurement using a three-electrode test cell at room temperature on a glassy carbon (GC) electrode (4 mm in diameter). The working electrode was a thin layer of Nafion-bonded catalyst cast on a rotating disk electrode (RDE). A Pt foil located in a separated compartment was used as the counter electrode, and a normal hydrogen electrode (NHE) was used as the reference electrode.

The electrolytes were 0.5 M  $\text{HClO}_4$  solutions with or without methanol. Ultra-pure oxygen was bubbled to maintain an oxygen-saturated atmosphere near the working electrode. The thin film on the GC electrode was prepared as follows: 5 mg of Pd/HPMo–PAN–C catalyst, 10 ml of ethanol and 50  $\mu\text{l}$  of 5% Nafion solution (DuPont) were mixed and ultrasonicated for 30 min to form a black catalyst ink. A 25  $\mu\text{l}$  aliquot of the ink was cast on the GC electrode surface. The coating was dried in air at room temperature for 1 h. The RDE curves were obtained in the acid solution under rotation at a scan rate of  $5 \text{ mV s}^{-1}$ . Cyclic voltammetry (CV) experiments were conducted in 0.5 M  $\text{HClO}_4$  as an electrolytic solution at a scanning rate of  $25 \text{ mV s}^{-1}$  with  $\text{N}_2$  purging. The hydrogen peroxide reduction experiments were performed in the 0.5 M  $\text{HClO}_4$  electrolyte containing either 0.1 M or 0.2 M hydrogen peroxide. The catalyst stability was evaluated by recording the current densities at 0.85 V (vs. NHE) in RDE curves after 1–100 scanning voltammetry cycles.

## 3. Results and discussion

The principle behind the synthesis of the Pd/HPMo–PAN–C catalyst is shown in Fig. 1. PAN provides a favorable combination of aromatic rings, similar to the crystalline structures of the carbon support. In step A, PAN is incorporated into the graphite of the carbon support due to the  $\pi$ – $\sigma$  interaction between PAN and the basal plane of the graphite [7]. In step B, protons are absorbed onto PAN–C in acidic media because of the alkalinity of PAN, forming a positive charge on the support surface. Because the HPMo composite has three negative charges,  $[\text{PMo}_{12}\text{O}_{40}]^{3-}$  can be immobilized on the PAN–C surface by impregnation due to the electrostatic interaction between  $\text{H}^+$  and  $[\text{PMo}_{12}\text{O}_{40}]^{3-}$  anions in step C, as described elsewhere [8].

Fig. 2 shows typical TEM micrographs for the Pd/HPMo–PAN–C and Pd/C catalysts. As shown in Fig. 2b, no obvious PAN layer or HPMo species are observed in the TEM image of the Pd/HPMo–PAN–C catalyst. The PAN content on the XC-72R carbon support is approximately 1 wt.% according to the synthetic procedure; therefore, the PAN layer on the carbon surface is too thin to be observed by TEM. The HPMo species is absorbed on the surface in the form of  $\text{PMo}_{12}\text{O}_{40}^{3-}$  instead of a cluster, so it is barely visible in Fig. 2b. For Pd/HPMo–PAN–C (Fig. 2b), the average nano-particle size is 2.1 nm and no agglomeration is observed on the HPMo–PAN–C support. For the Pd/C catalyst, the average particle size is 4.3 nm and Pd nano-particle agglomeration is apparent (Fig. 2a). HPMo can be irreversibly adsorbed on metal surfaces [8]. When the Pd precursors are reduced to metallic Pd, the resultant Pd nano-particles are evenly deposited on the HPMo–PAN–C supports due

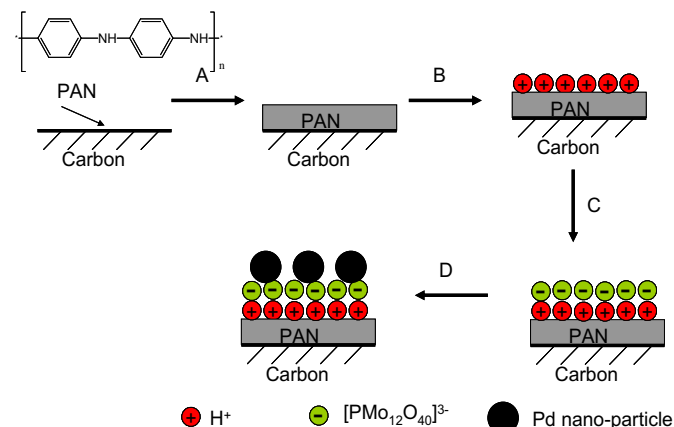


Fig. 1. The principle behind the synthesis of the Pd/HPMo–PAN–C catalyst.

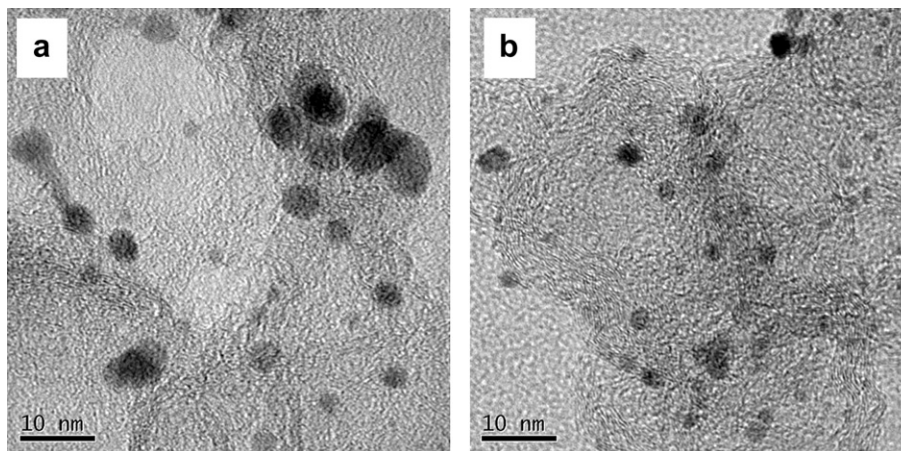


Fig. 2. TEM images of (a) Pd/C and (b) Pd/HPMo-PAN-C catalysts.

to the strong interaction between Pd and HPMo. The presence of HPMo species may inhibit the agglomeration of Pd nano-particles by acting as a protective agent.

FTIR experiments were conducted to confirm the presence of PAN and HPMo in the Pd/HPMo-PAN-C catalyst. In Fig. 3a, the characteristic PAN absorption peaks are observed at 1230, 1300, 1478, 1584 and 2938  $\text{cm}^{-1}$ , corresponding to the C=N stretch, the C-N stretch, the quinoid ring vibration, the benzenoid ring vibration and the  $\text{CH}_2$  stretch, respectively [9,10]. The four clear peaks at 1065, 968, 869, and 790  $\text{cm}^{-1}$  are assigned to the inner P-O-Mo bond, external Mo=O bond, Mo-O<sub>b</sub>-Mo bridge and Mo-O<sub>c</sub>-Mo bridges, respectively [11]. The FTIR results indicate the presence of PAN and HPMo in the Pd/HPMo-PAN-C catalyst and that HPMo species retains its Keggin structure. The stability of HPMo in the Pd/HPMo-PAN-C catalyst is assessed by FTIR after the sample is impregnated in 0.5 M  $\text{HClO}_4$  solution for 12 h. Fig. 3b shows that the characteristic bands associated with HPMo for the Pd/HPMo-PAN-C catalyst are essentially the same both before and after the impregnation in acid medium. This result clearly indicates that the HPMo immobilized on the carbon support is very stable and does not leach out in 0.5 M  $\text{HClO}_4$  solution even though free HPMo is soluble in water. The excellent stability of HPMo in the catalyst may be attributed to the strong electrostatic interaction between the positive charge of the support and the  $[\text{PMo}_{12}\text{O}_{40}]^{3-}$  anions, as mentioned above.

Typical XRD patterns of carbon support, PAN-C and HPMo-PAN-C are shown in Fig. 4a. For these three samples, the peaks at approximately  $24.5^\circ$  and  $43.5^\circ$  are attributed to the diffraction of (002) and (100) plane of the hexagonal structure of the carbon support. In the pattern of HPMo-PAN-C sample, the shoulder peak at  $2\theta = 20.6^\circ$  can be assigned to the diffraction of PAN [12] and the broad peaks from  $40^\circ$  to  $60^\circ$  are attributed to the presence of HPMo species, which are well dispersed on the support surface. The XRD patterns of Pd/HPMo-PAN-C and Pd/C are compared in Fig. 4b. The diffraction peaks at approximately  $39^\circ$ ,  $46^\circ$ ,  $68^\circ$ , and  $81^\circ$  in these two catalysts are due to the Pd (111), (200), (220) and (311) planes, respectively, which are typical of a crystalline Pd face-centered cubic pattern. With the addition of HPMo, the diffraction peaks of the Pd/HPMo-PAN-C catalyst shift to lower angles than those of Pd/C. This shift may be attributed to the interaction between Pd and  $\text{MoO}_x$  species on the support, which causes the increment of the crystalline lattice of Pd [13,14]. The Scherrer formula [15] can be used to calculate the metal particle size from the fitted (220) plane, yielding Pd/HPMo-PAN-C and Pd/C particle sizes of 4.7 nm and 11.8 nm, respectively. The particle size of Pd/HPMo-PAN-C is somewhat smaller than that of Pd/C, which is consistent with the TEM results.

The ORR catalytic activity and methanol selectivity tolerance of Pd/HPMo-PAN-C was compared with those of the Pt/C catalyst (20 wt.% Pt loading, purchased from Johnson Matthey), and the results were displayed in Fig. 5. Fig. 5a shows the ORR catalytic activity of Pd/HPMo-PAN-C, Pd/C, HPMo-PAN-C and Pt/C in

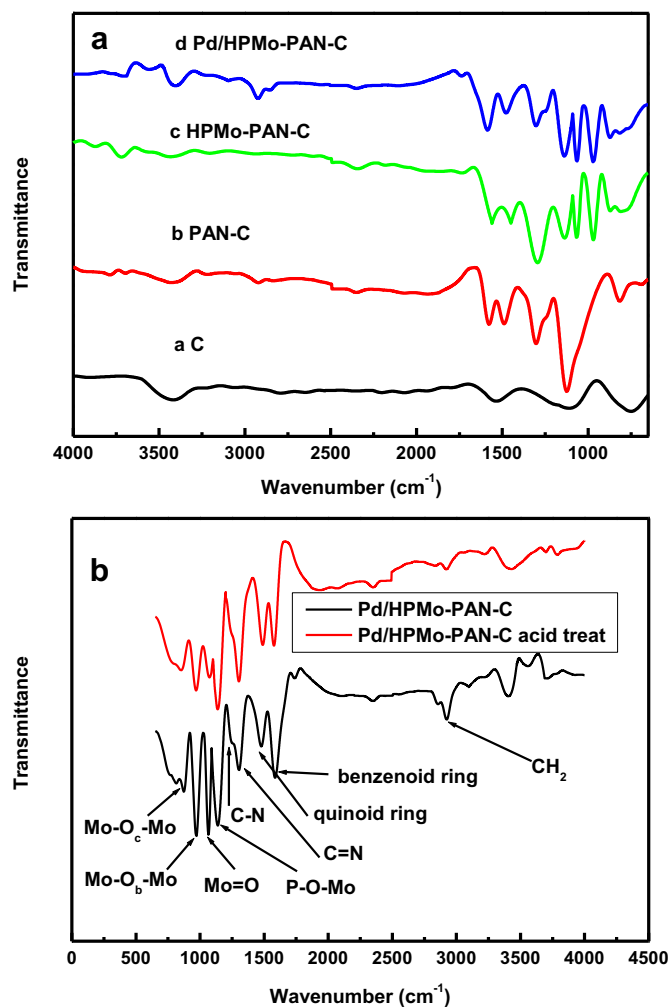


Fig. 3. (a) FTIR spectra of C, PAN-C, HPMo-PAN-C and Pd/HPMo-PAN-C. (b) FTIR spectra of the Pd/HPMo-PAN-C catalyst before and after 12 h of treatment in 0.5 M  $\text{HClO}_4$  solution.

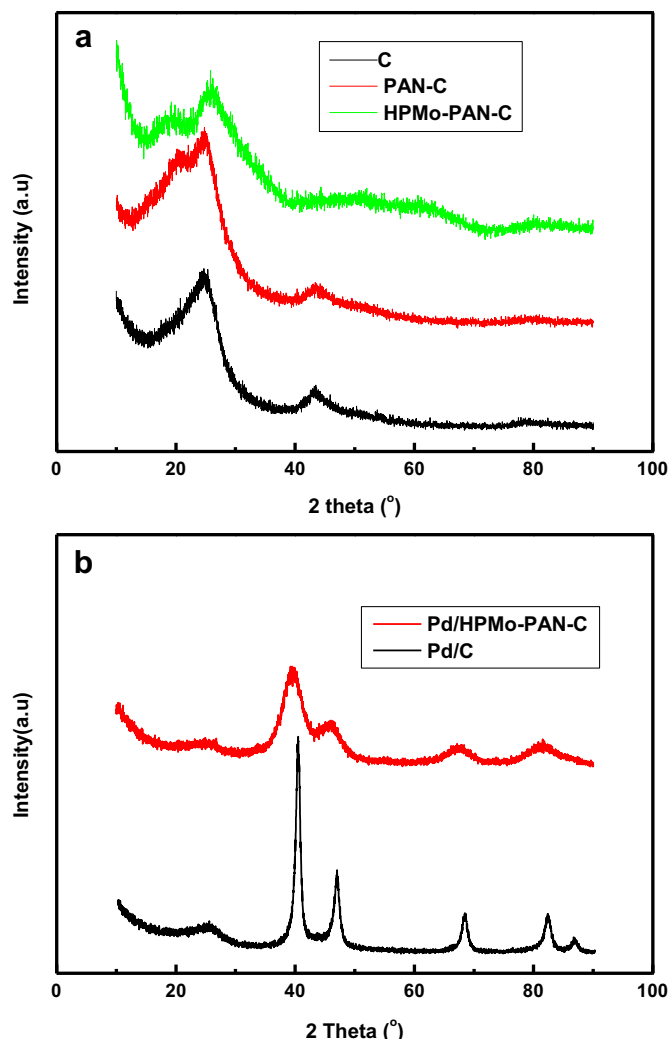


Fig. 4. XRD patterns of (a) C, PAN-C, HPMo-PAN-C, (b) Pd/HPMo-PAN/C and Pd/C.

O<sub>2</sub>-saturated HClO<sub>4</sub> solution with an electrode rotation speed of 1600 rpm. In Fig. 5a, the HPMo-PAN-C sample shows almost no catalytic activity for ORR. Pd/C displays poor catalytic activity in the potential range from 0.95 to 0.7 V (vs. NHE), in which a fuel cell cathode is expected to work. At a potential of 0.85 V (vs. NHE), the ORR current density for the Pd/C catalyst is approximately 0.29 mA cm<sup>-2</sup>, whereas that for Pd/HPMo-PAN-C is approximately 1.01 mA cm<sup>-2</sup>, which is very close to the 1.32 mA cm<sup>-2</sup> current density exhibited by the Pt/C sample. Fig. 5b compares Pd/HPMo-PAN-C, Pd/C and Pt/C in O<sub>2</sub>-saturated HClO<sub>4</sub> solution in the presence of 1 M CH<sub>3</sub>OH. For Pt/C, methanol oxidation begins at 0.9 V (vs. NHE) and peaks at approximately 0.7 V (vs. NHE). Next, the combined results of methanol oxidation and ORR lead to a slightly higher limiting current density, which is much lower than that obtained in 0.5 M HClO<sub>4</sub> solution without methanol. This finding indicates that in the fuel cell operation mode, when Pt/C is adopted as the cathode catalyst, the permeated methanol from the anode will decrease the cell performance due to the mixed potential formed at the cathode. However, for Pd/HPMo-PAN-C and Pd/C under the same operating conditions, the addition of methanol to 0.5 M HClO<sub>4</sub> solutions has almost no effect on the ORR activity, which is consistent with the literature [1,16]. This result suggests that the as-prepared Pd/HPMo-PAN-C exhibits both comparable performance for ORR with respect to Pt/C and an excellent

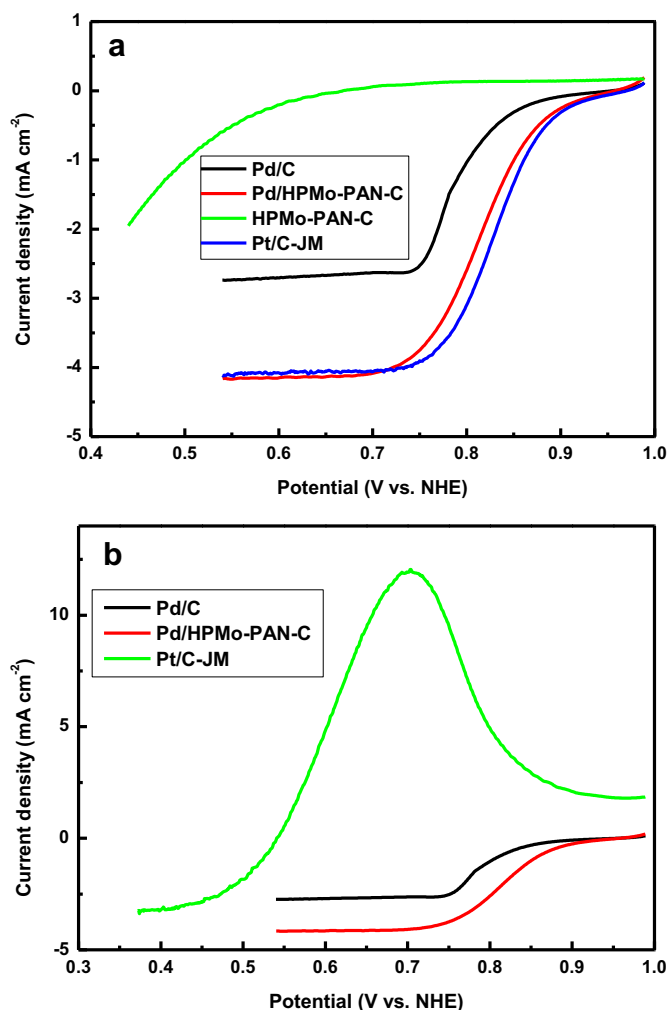
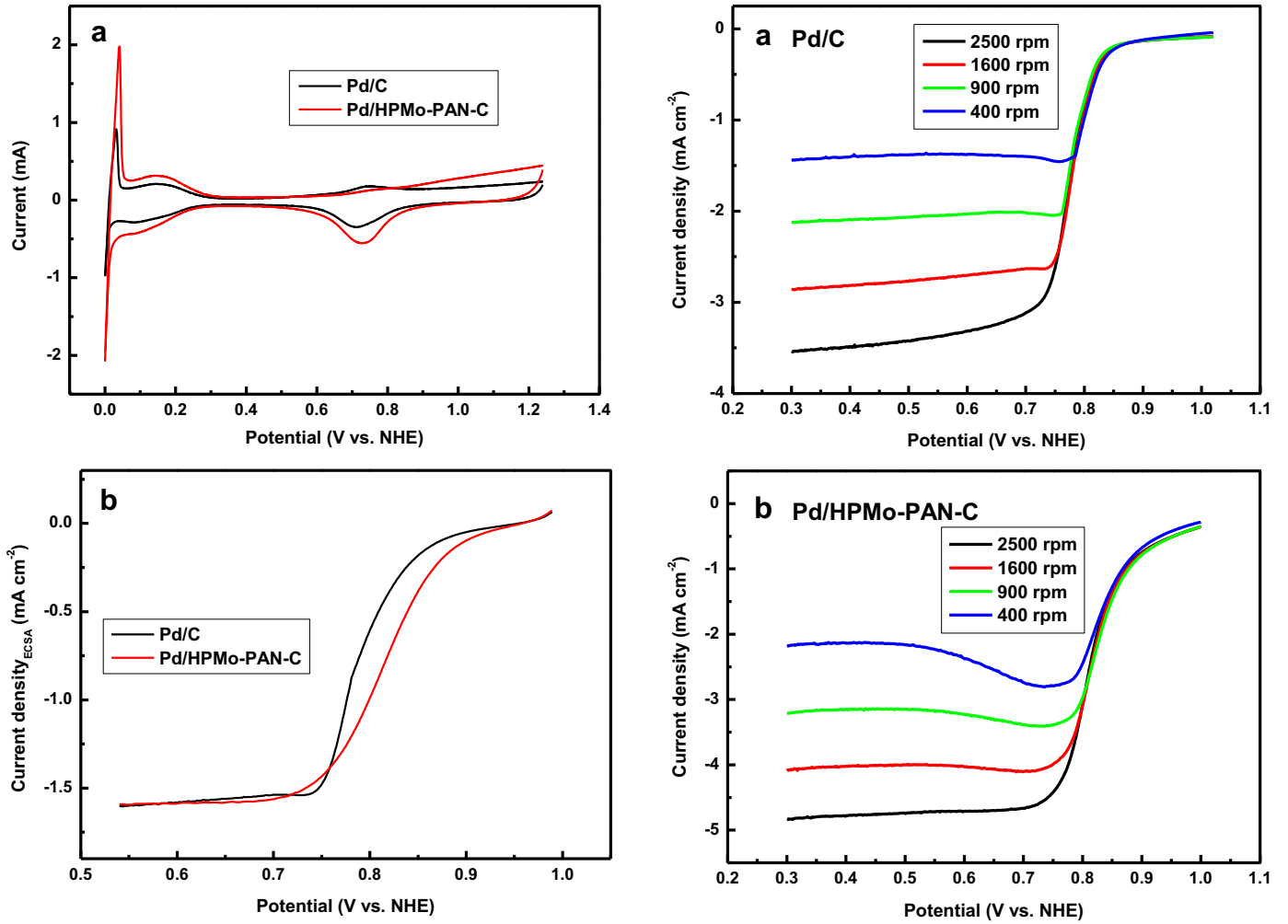


Fig. 5. (a) Polarization curves for the ORR on Pd/C, Pd/HPMo-PAN-C, Pt/C-JM and HPMo-PAN-C samples in 0.5 M HClO<sub>4</sub> with sweeping rate of 5 mV s<sup>-1</sup> and a rotating speed of 1600 rpm. (b) Polarization curves for the ORR over Pt/C-JM and Pd/HPMo-PAN-C catalysts in oxygen-saturated 0.5 M HClO<sub>4</sub> in the presence of 1 M CH<sub>3</sub>OH. Rotation rate: 1600 rpm; sweep rate: 5 mV s<sup>-1</sup>.

tolerance to methanol oxidation, which is quite interesting and attractive for use as the cathode catalyst of DMFC.

Pd/C and Pd/HPMo-PAN-C catalysts have different average particle sizes. Therefore, the active sites provided by these two catalysts will influence their catalytic activity towards ORR. To elucidate the increase in the catalytic activity caused by the HPMo species, the ORR currents of Pd/C and Pd/HPMo-PAN-C must be measured and normalized by their electro-chemical surface areas (ECSA). To determine the ECSA of the obtained Pd/C and Pd/HPMo-PAN-C catalyst, we performed CV experiments in 0.5 M HClO<sub>4</sub> as an electrolytic solution at a scanning rate of 25 mV s<sup>-1</sup> with N<sub>2</sub> purging. As shown in Fig. 6a, the CV curves exhibit two distinctive potential regions associated with hydrogen adsorption and desorption. The charge involved in hydrogen under potential deposition (H<sub>upd</sub>) in the potential window of 0.05 V–0.31 V (vs. NHE) is used to estimate ECSA of the catalysts [17]. The H<sub>upd</sub> charge is converted into ECSA using the specific charge of 212 μC cm<sup>-2</sup> associated with the H<sub>upd</sub> on pure Pd surfaces. The ECSA values were 34.2 m<sup>2</sup> g<sup>-1</sup> and 52.3 m<sup>2</sup> g<sup>-1</sup> for Pd/C and Pd/HPMo-PAN-C catalysts, respectively. The specific activity of Pd/C and Pd/HPMo-PAN-C are normalized by their ECSA values, and the results are shown in Fig. 6b. From Fig. 6b, it can be observed that the limiting diffusion current densities of Pd/C and





**Fig. 6.** (a) Cyclic voltammograms for Pd/HPMo-PAN-C and Pd/C in 0.5 M HClO<sub>4</sub> electrolyte. Scanning rate: 5 mV s<sup>-1</sup>. (b) Specific ORR activity normalized by ECSA for the Pd/C and Pd/HPMo-PAN-C catalysts. Rotation rate: 1600 rpm; sweep rate: 5 mV s<sup>-1</sup>; Pd loading: 10 μg cm<sup>-2</sup>.

Pd/HPMo-PAN-C are very close. At the potential of 0.85 V (vs. NHE), the specific activity of Pd/HPMo-PAN-C to ORR is approximately 0.38 mA cm<sup>-2</sup>, which is close to the results for Pt/C reported in the literature [18]. The ORR curve of the Pd/HPMo-PAN-C catalyst is 30 mV more positive than that of the Pd/C catalyst. This result shows that the addition of HPMo promotes the ORR performance of Pd nano-particles.

To investigate the effect of HPMo species on the ORR mechanism of Pd nano-particles, rotating disk electrodes of Pd/HPMo-PAN-C and Pd/C in 0.5 M HClO<sub>4</sub> solution were tested at different rotating speeds. The results are shown in Fig. 7. From Fig. 7a and b, the limiting currents density are observed for potentials below 0.7 V (vs. NHE) for both samples, indicating that diffusion is the dominant step in the ORR process at those potentials. With increasing electrode rotation rate, the limiting current densities are increased, indicating that the dominant step of ORR is associated with the convective of oxygen in the solution at the potential value of 0.7 V (vs. NHE). According to Koutecky-Levich theory [19], the disk current density ( $I_d$ ) on the electrode can be expressed by the following equations:

$$\frac{1}{I_d} = \frac{1}{I_{lev}} + \frac{1}{I_k} \quad (1)$$

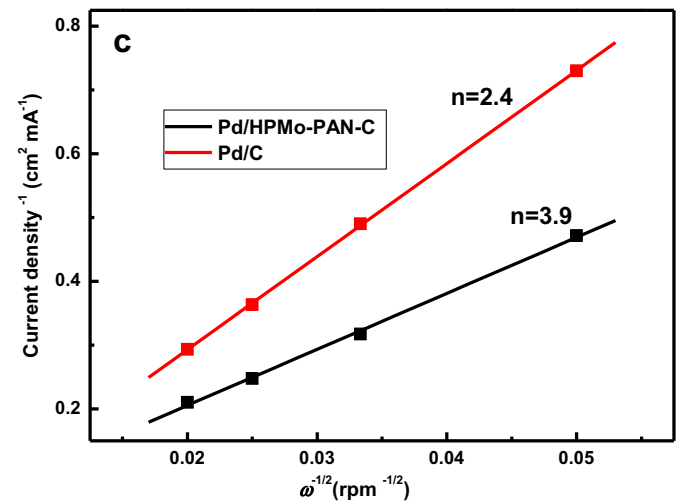


**Fig. 7.** Polarization curves for the ORR on (a) Pd/C and (b) Pd/HPMo-PAN-C samples in oxygen-saturated 0.5 M HClO<sub>4</sub> with electrode rotating speeds of 400, 900, 1600 and 2500 rpm. (c) Levich plots for the ORR on Pd/C and Pd/HPMo-PAN-C catalysts. Current density was measured at 0.7 V (vs. NHE).

$$I_{lev} = 0.62nFC_{O_2}D_{O_2}^{2/3}\nu^{-1/6}\omega^{1/2} \quad (2)$$

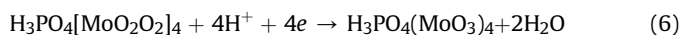
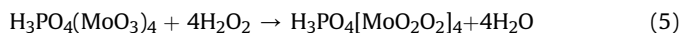
where  $I_{lev}$  is the Levich diffusion current,  $n$  is the overall electron transfer number in the ORR,  $F$  is the Faraday constant

( $96,487 \text{ C mol}^{-1}$ ),  $C_{O_2}$  is the oxygen concentration in the aqueous solution ( $1.13 \times 10^{-5} \text{ M}$ ),  $D_{O_2}$  is the  $O_2$  diffusion coefficient ( $1.93 \times 10^{-6} \text{ cm}^2 \text{ s}^{-1}$ ),  $\nu$  is the kinetic viscosity of the solution ( $0.01 \text{ cm}^2 \text{ s}^{-1}$ ), and  $\omega$  is the electrode rotation rate (rpm). Based on these two equations,  $I_d$  possesses the same line slope with  $I_{lev}$ , therefore, the electron transfer number in ORR process can be calculated using the line slopes of the plots of  $1/I_d$  vs.  $\omega^{-1/2}$ . Fig. 7c shows that the electron transfer numbers in ORR are 2.4 and 3.9 for Pd/C and Pd/HPMo–PAN–C, respectively. This result indicates that the HPMo species enhance the catalytic activity of Pd nano-particles by increasing the electron transfer component of ORR.

The significant enhancement in the ORR catalytic activity of Pd/HPMo–PAN–C catalysts compared to Pd/C catalysts may be attributed to two effects: first, the more uniform distribution and smaller particle size of the Pd nano-particles on the HPMo–PAN–C support surface, as indicated by TEM, provide more active sites for the ORR process; second, the presence of HPMo species promotes the ORR electron transfer, as presented in Fig. 7c. In the ORR process, two reactions occur on the catalyst surface, as described in equations (3) and (4):



Hydrogen peroxide is the intermediate species when ORR proceeds via the two-electron pathway [20]. The electron transfer number for the Pd/C catalyst is 2.4; therefore, hydrogen peroxide is the main product in Pd/C-catalyzed ORR. In the case of the obtained Pd/HPMo–PAN–C catalyst, due to the presence of HPMo with a Keggin structure, peroxo bonds can be formed in HPMo as soon as hydrogen peroxide is produced, as shown by equation (5) [21]. Therefore, the addition of HPMo may promote the decomposition of hydrogen peroxide and enhance the catalytic activity of Pd nano-particles for ORR by increasing the electron transfer number. The peroxo HPMo species produced in equation (5) is not stable and can be reduced to HPMo to recycle the catalysts, as shown in equation (6).



To verify the assumption that HPMo promotes the decomposition of ORR-produced hydrogen peroxide, the polarization curves of HPMo–PAN–C and XC-72R carbon were measured in a 0.5 M  $HClO_4$  electrolyte containing 0.1 M hydrogen peroxide. Fig. 8a shows that the HPMo–PAN–C catalyst begins hydrogen peroxide reduction at potentials as positive as 0.8 V (vs. NHE) and that the current density is more positive than that of XC-72 carbon. This result indicates that HPMo–PAN–C is active for the reduction of hydrogen peroxide in acidic media. It must be noted that HPMo–PAN–C exhibits an oxidized current in the potential region from 0.4 V to 0.6 V (vs. NHE), which may be attributed to the oxidation of HPMo, as described by equation (5). Fig. 8b shows the CV curves for the HPMo–PAN–C samples in 0.5 M  $HClO_4$  containing different hydrogen peroxide concentrations. The reduction current density of hydrogen peroxide increases significantly when the hydrogen peroxide concentration in the electrolyte increases from 0 M to 0.02 M. The results of Fig. 8 indicate that HPMo species promote hydrogen peroxide decomposition. Similar phenomena were also reported by other researchers. J.L. Fernandez and Luque [22] found that molybdenum phosphate promoted hydrogen peroxide decomposition by testing CV curves in the electrode with different hydrogen peroxide concentrations. P.J. Kulesza et al. [5] reported

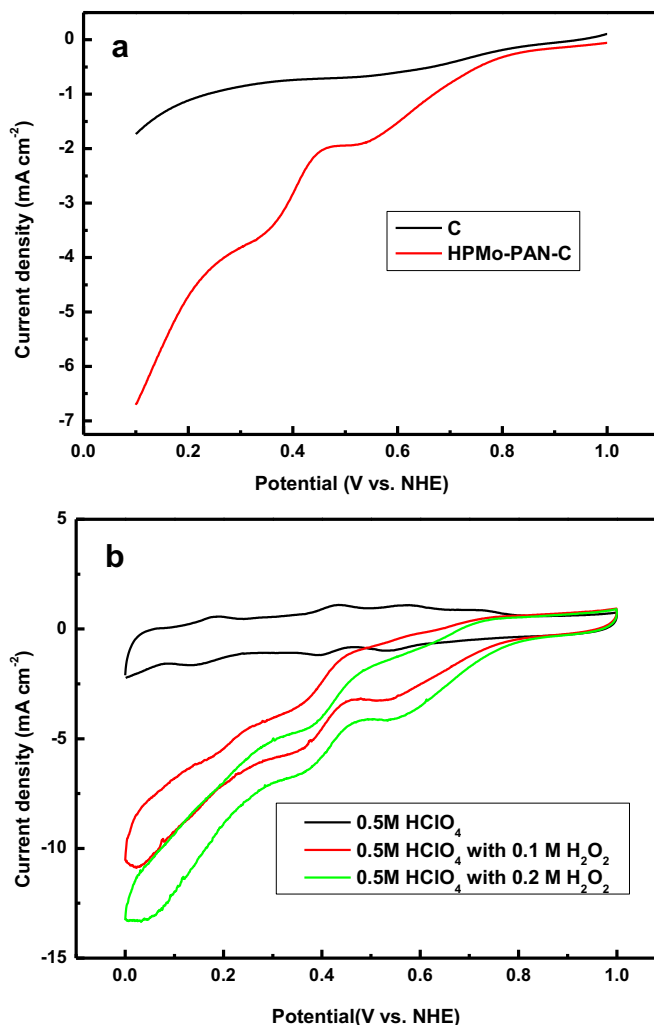


**Fig. 8.** (a) Polarization curves for hydrogen peroxide reduction on XC-72R carbon and HPMo–PAN–C samples in 0.5 M  $HClO_4$  containing 0.1 M hydrogen peroxide with a sweeping rate of  $5 \text{ mV s}^{-1}$  and rotating speed of 1600 rpm. (b) Cyclic voltammograms for HPMo–PAN–C samples in 0.5 M  $HClO_4$  electrolyte containing 0 M, 0.1 M and 0.2 M hydrogen peroxide. Scanning rate:  $10 \text{ mV s}^{-1}$ ,  $\omega$ : 1600 rpm.

that HPMo deposited on Pt catalysts exhibited catalytic activity towards hydrogen peroxide reduction and thus facilitated electron transfer in ORR.

To investigate the stability of the obtained Pd/HPMo–PAN–C catalyst, the current densities of ORR on the catalyst surface were recorded at 0.85 V (vs. NHE) after 1–100 cyclic voltammetry scanning cycles. The Pd/HPMo–C catalyst prepared by directly impregnating HPMo on the carbon support was also evaluated for comparison. As shown in Fig. 9, the current density of Pd/HPMo–C at 0.85 V (vs. NHE) decreases from  $0.99 \text{ mA cm}^{-2}$  to  $0.28 \text{ mA cm}^{-2}$  after 20 scanning cycles. The decrease in the ORR catalytic activity may be attributed to the dissociation of HPMo in the  $HClO_4$  solution during the scanning process. However, the current density of the Pd/HPMo–PAN–C catalyst decreases from  $1.01 \text{ mA cm}^{-2}$  to  $0.91 \text{ mA cm}^{-2}$  even after 100 scanning cycles. This result shows that Pd/HPMo–PAN–C catalyst has excellent stability in acid media. As discussed above, the enhanced ORR catalytic activity of the Pd nano-particles is attributed to the presence of HPMo species on the surface of the carbon support; thus, the stability of Pd/HPMo–PAN–C indicates that the HPMo species is not easily dissociated from the carbon support in acid media, which is consistent with the FTIR results in Fig. 3b.

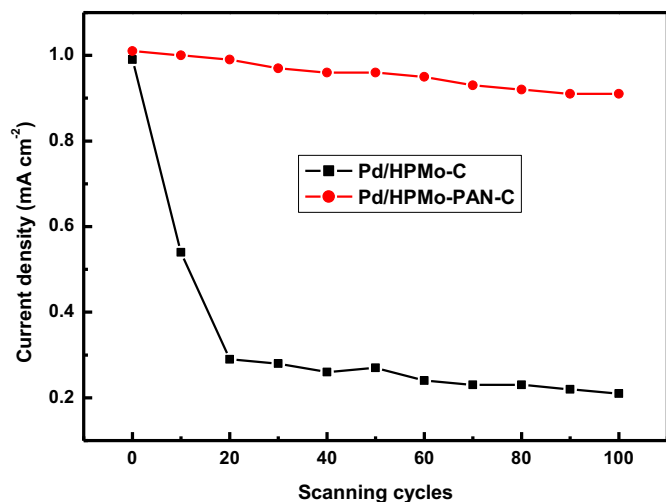


Fig. 9. Effect of scanning cycles on the ORR current density of Pd/HPMo–C and Pd/HPMo–PAN–C. Current density was measured at 0.85 V (vs. NHE).

#### 4. Conclusion

In the synthesis of the Pd/HPMo–PAN–C catalyst, the addition of HPMo to the carbon support is more convenient than the traditional electro-chemical deposition method. The presence of HPMo species in Pd/HPMo–PAN–C not only reduces the particle size of Pd nano-particles but also promotes the electron transfer number in the ORR process. Pd/HPMo–PAN–C exhibits higher ORR catalytic activity than that of Pd/C. The obtained Pd/HPMo–PAN–C shows excellent stability because the electronic interaction of HPMo and PAN decrease the dissociation of HPMo species in the  $\text{HClO}_4$  solution. Considering that Pd/HPMo–PAN–C is less expensive and has higher methanol tolerance than the Pt/C catalyst, the obtained Pd/HPMo–PAN–C catalyst may be applied as an effective catalyst in the DMFC cathode.

#### Acknowledgments

The authors would like to acknowledge the support of the National Basic Research Program (973 Program) of China (2010CB234605, 2012CB720302), the Doctor's Special Fund of Xinjiang Production and Construction Corps (2010JC13) and the Initial Fund for High-Level Talents of Shihezi University (RCZX20036).

#### References

- [1] M.H. Shao, K. Sasaki, R.R. Adzic, *J. Am. Chem. Soc.* 128 (2006) 3526–3527.
- [2] W.M. Wang, D. Zheng, C. Du, Z.Q. Zou, X.G. Zhang, B.J. Xia, H. Yang, D.L. Akins, *J. Power Sources* 167 (2007) 243–249.
- [3] M.H. Seo, S.M. Choi, H.J. Kim, J.H. Kim, B.K. Cho, W.B. Kim, *J. Power Sources* 179 (2008) 81–86.
- [4] D.L. Wang, S.F. Lu, Y. Xiang, S.P. Jiang, *Appl. Catal. B: Environ.* 103 (2011) 311–317.
- [5] M. Chojak, A.K. Zurowska, R. Włodarczyk, K. Miecznikowski, K. Karnicka, B. Palys, R. Marassi, P.J. Kulesza, *Electrochim. Acta* 52 (2007) 5574–5581.
- [6] D.L. Wang, S.F. Lu, Y. Xiang, S.P. Jiang, *Chem. Commun.* 46 (2010) 2058–2060.
- [7] G. Wu, K.L. More, C.M. Johnston, P. Zelenay, *Science* 332 (2011) 443–447.
- [8] P.J. Kulesza, M. Chojak, K. Karnicka, K. Miecznikowski, B. Palys, A. Lewera, *Chem. Mater.* 16 (2004) 4128–4134.
- [9] Y.C. Dong, Z.B. Han, C.Y. Liu, F. Du, *Sci. Total Environ.* 408 (2010) 2245–2253.
- [10] D.P. He, C. Zeng, C. Xu, N.C. Cheng, H.G. Li, S.C. Mu, M. Pan, *Langmuir* 27 (2011) 5582–5588.
- [11] D.P. Liu, X.Y. Quek, S.Q. Hu, L.S. Li, H.M. Lim, Y.H. Yang, *Catal. Today* 147S (2009) S51–S57.
- [12] J.G. Deng, X.B. Ding, W.C. Zhang, Y.X. Peng, J.H. Wang, X.P. Long, P. Li, A.S.C. Chan, *Eur. Polym. J.* 38 (2002) 2497–2501.
- [13] C.W. Kuo, C. Sivakumar, T.C. Wen, *J. Power Sources* 185 (2008) 807–814.
- [14] E.I. Santiago, G.A. Camara, E.A. Ticianelli, *Electrochim. Acta* 48 (2003) 3527–3534.
- [15] V. Radmilovic, H.A. Gasteiger, P.N. Ross, *J. Catal.* 154 (1995) 98–106.
- [16] S. Tominaka, T. Momma, T. Osaka, *Electrochim. Acta* 53 (2008) 4679–4686.
- [17] S. An, J. Park, C. Shin, J. Joo, E. Ramasamy, J. Hwang, J. Lee, *Carbon* 49 (2001) 1108–1117.
- [18] W.Z. Li, P. Haldar, *Electrochem. Commun.* 11 (2009) 1195–1198.
- [19] P.J. Kulesza, B. Grzybowska, M.A. Malik, M.T. Galkowski, *J. Electrochem. Soc.* 144 (1997) 1911–1917.
- [20] C.M. Sanchez, A.J. Bard, *Anal. Chem.* 81 (2009) 8094–8100.
- [21] Z.W. Xi, N. Zhou, Y. Sun, K.L. Li, *Science* 292 (2001) 1139–1141.
- [22] G.C. Luque, J.L. Fernandez, *J. Power Sources* 203 (2012) 57–64.